Mediator-free interaction of glucose oxidase, as model enzyme for immobilization, with Al-doped and undoped ZnO thin films laser-deposited on polycarbonate supports

Journal Item

Title: Mediator-free interaction of glucose oxidase, as model enzyme for immobilization, with Al-doped and undoped ZnO thin films laser-deposited on polycarbonate supports

Author: Fidal V.T.K.P. Saikumar Inguva Satheesh Krishnamurthy Enrico Marsili Jean-Paul Mosnier Chandra T.S.

PII: S0141-0229(16)30185-5
DOI: http://dx.doi.org/doi:10.1016/j.enzmictec.2016.09.012
Reference: EMT 8982

To appear in: *Enzyme and Microbial Technology*

Received date: 13-5-2016
Revised date: 19-9-2016
Accepted date: 21-9-2016

Please cite this article as: V.T.K.P.Fidal, Inguva Saikumar, Krishnamurthy Satheesh, Marsili Enrico, Mosnier Jean-Paul, T.S.Chandra.Mediator-free interaction of glucose oxidase, as model enzyme for immobilization, with Al-doped and undoped ZnO thin films laser-deposited on polycarbonate supports.*Enzyme and Microbial Technology* http://dx.doi.org/10.1016/j.enzmictec.2016.09.012

Mediator-free interaction of glucose oxidase, as model enzyme for immobilization, with Al-doped and undoped ZnO thin films laser-deposited on polycarbonate supports

Fidal V T K P[a], Saikumar Inguva[b], Satheesh Krishnamurthy [b,#], Enrico Marsili[d,*], Jean-Paul Mosnier[b], Chandra T S [a].

[a]Bhupat and Jyoti Mehta School of Biosciences, Department of Biotechnology, Indian Institute of technology, Madras, Chennai-600036, India

[b]School of Physical Sciences and National Centre for Plasma Science and Technology, Dublin City University, Collins Avenue, Dublin9, Ireland

[d] School of Biotechnology, Dublin City University, Collins Avenue, Dublin9, Ireland

[#]*Present address*: Department of Engineering and Innovation Materials Engineering, Open University, UK-MK7 6AA

[*]*Present address*: Singapore Centre for Life Sciences Engineering, Nanyang Technological University, 60 Nanyang drive, 637551 Singapore

Research Highlights:

- Electrochemical interaction of ZnO and AZO thin films with the enzyme glucose oxidase was studied.
- Nature of interaction of GOx with AZO was explored using XPS.
- Mechanism of the electron transfer between GOx and AZO/ZnO was studied using EIS.
- The results show that AZO is preferable to ZnO for GOx immobilization and glucose sensor development.

Abstract:

Al doped and undoped ZnO thin films were deposited by pulsed-laser deposition on polycarbonate sheets. The films were characterized by optical transmission, Hall effect measurement, XRD and SEM. Optical transmission and surface reflectometry studies showed good transparency with thicknesses ~100 nm and surface roughness of 10 nm. Hall effect measurements showed that the sheet carrier concentration was -1.44 x 10^{15} cm^{-2} for AZO and -6 x 10^{14} cm^{-2} for ZnO. The films were then modified by drop-casting glucose oxidase (GOx) without the use of any mediators. Higher protein concentration was observed on ZnO as compared to AZO with higher specific activity for ZnO (0.042 U mg^{-1}) compared to AZO (0.032 U mg^{-1}), and was in agreement with cyclic voltemmetry (CV). X-ray photoelectron spectroscopy (XPS) suggested that the protein was bound by dipole interactions between AZO lattice oxygen and the amino group of the enzyme. Chronoamperometry showed sensitivity of 5.5 μA mM^{-1} cm^{-2} towards glucose for GOx/AZO and 2.2 μA mM^{-1} cm^{-2} for GOx/ZnO. The limit of detection (LoD) was 167 μM of glucose for GOx/AZO, as compared to 360 μM for GOx/ZnO. The linearity was 0.28-28 mM for GOx/AZO whereas it was 0.6-28 mM for GOx/ZnO with a response time of 10s. Possibly due to higher enzyme loading, the decrease of impedance in presence of glucose was larger for GOx/ZnO as compared to GOx/AZO in electrochemical impedance spectroscopy (EIS). Analyses with clinical blood serum samples showed that the systems had good reproducibility and accuracy. The characteristics of novel ZnO and AZO thin films with GOx as a model enzyme, should prove useful for the future fabrication of inexpensive, highly sensitive, disposable electrochemical biosensors for high throughput diagnostics.

Keywords*: Glucose oxidase, ZnO, Al-doped ZnO, Polycarbonate*

1. Introduction

ZnO is a well-established material for bio-sensing applications due to its unique features such as high catalytic efficiency, bio-compatibility, strong adsorbance, electrochemical activity, easy availability and long term stability [1–3]. It has other advantages over other metal oxide thin films, including the possibility of low temperature deposition, facile fabrication of nanostructures and attractive optoelectronic and piezoelectric properties[4,5].

Doping is a common method to alter the electronic and optical properties of ZnO thin films[6]. Aluminum (Al) and gallium (Ga) are n-type dopants that increase the concentration of free electrons, thereby improving the conductivity of ZnO films [7,8]. Al-doping of ZnO (AZO) had shown higher reactivity and optical transmittance than ZnO and is preferred dopant for the fabrication of transducer devices[8,9]. The resistivity is dependent not only on the Al concentration but also on the oxygen partial pressure used during the plasma assisted deposition[10]. Aragones et al (2013) reported that doping ZnO with increasing concentrations of Al (2-11 at %) increased the carrier concentration from 10^{19} to 7 x 10^{20} cm^{-3} [11]. Al doped ZnO is more sensitive as compared to undoped ZnO towards adsorbed species on the surface. Therefore doping of ZnO has a wide application in gas and humidity sensors [12,13].

Effect of doping on the immobilization of enzyme and their activity remains largely unexplored. Changes in the surface charge due to introduction of the dopants might result in altered quantity of the enzyme immobilized on the surface and consequently the overall activity of the system.

Conventional electrode supports such as gold and Pt are expensive and difficult to fabricate [14]. Most of the electrodes involving the use of metal oxides have expensive indium tin oxide (ITO) as base electrode with mediators [15–17]. The major drawback in using ITO is indium migration during operation [18]. Therefore, there is a need for alternative materials as electrode support, with advantageous properties. Saha and Gupta reported Al- and Fe co-doped ZnO conductive biosensors on glass, avoiding the need for a support electrode [14]. In this work, we have used polycarbonate (PC) plastic as a base material to grow thin metal oxide films as compared to conventional ITO base [15]. PC features high optical transparency (90%), temperature compatibility (145 °C), low-water absorption (0.2-0.35%) and relatively low cost. The deposition of high quality films needs to be carried out around 100 °C because the glass transition temperature of PC is close to 145 °C. In addition PC is an easily maneuverable, light weight material which can be cut to exact required dimensions. The pulsed laser deposition (PLD) technique meets this requirement. PLD allows room/low temperature deposition of crystalline ZnO/AZO materials, produces low energy plasma particles that do not damage the plastic substrates and maintains the stoichiometry of the initial target material [19,20].

Glucose oxidase (GOx) is a widely studied redox protein used extensively for the fabrication of glucose sensors. It is a dimer of 160 kDa with flavin adenine dinucleotide (FAD) as the co-enzyme [21]. GOx presents two possible electron transfer mechanisms, one through the

breakdown of the by-product hydrogen peroxide and the other through the direct electron transfer from $FADH_2$. The mechanism at play varies depending upon the distance between the catalytic site on the surface of the electrode and the mediator used in the buffer [22]. Because of these well-known properties, GOx is an ideal model enzyme for studying the electron transfer pathway for new material interfaces such as ZnO/PC. Especially, ZnO has a high iso-electric point of 9.3, which provides a suitable interface for GOx with an iso-electric point of 4.5 [2]. As the GOx electron transfer mechanism depends on the distance between the catalytic site and the surface charges on the electrode, it was interesting to investigate how this may influence the reactivity of GOx immobilized on ZnO/PC or AZO/PC to glucose without a mediator.

In this work high quality transparent and conductive ZnO and AZO films were obtained by PLD deposition on PC. The deposits were optimized by using different Al concentration and oxygen pressure conditions. The change in GOx activity on immobilization on the doped surface was explored. Since PC based ZnO films can perform as inexpensive, flexible and disposable electrodes, their usefulness for biosensing was validated by carrying out glucose tests with blood serum samples.

2. Experimental Details

2.1 Thin films deposition and characterization

ZnO and AZO thin films were prepared by PLD using a high-power, Q-switched, frequency-quadrupled, Nd:YAG laser. The laser specifications were 266 nm wavelength, 150 mJ laser energy, 2 Jcm^{-2}average fluence, 10 Hz repetition rate and 6 ns pulse width [13].Rectangular sheets of 1 cm × 2 cm and 1.2 mm thick polycarbonate (Lexan 9030) were used as substrates. Prior to deposition the substrates were cleaned with isopropyl alcohol and then dried in nitrogen gas. The deposition chamber was pumped down to the base pressure of 3×10^{-5} mTorr (~ 4×10^{-6} Pa) for all the depositions. The oxygen pressure in the chamber was kept at 10 mTorr (~ 1.3 Pa) and 30 mTorr (~ 4 Pa) for the ZnO and AZO thin films respectively. The substrate temperature was raised to 100 °C and kept constant for the whole deposition. Ten thousand laser shots were used for the 15 minutes long depositions, after which the substrate temperature was lowered to 30 °C.

The surface morphology was studied by scanning electron microscopy (FEG Quanta 400F). XRD was used to establish the crystalline structure of the samples using Bruker Discover D8. Optical transmission spectra were recorded using Jasco UV/VIS/IR spectrophotometer with a scan rate of 200 nm min^{-1} and band width of 2 nm. Surface reflectometry was carried out at an angle of 70º and a wavelength of 628 nm (JA Woolman surface reflectometer).The electrical properties such as sheet resistance and carrier concentration were measured using a four-point probe/ Hall effect instrument (Accent HL5500).

2.2 Glucose oxidase immobilization:

A stock solution of 2mg mL^{-1} of GOx was prepared in phosphate buffer (pH 7.2). This solution (2.5 µL) was dropped on a 0.25 cm^2 (0.5 cm x 0.5 cm) area of a thin film of size 0.35 cm^2 (0.7 x 0.5 cm). To ensure uniform spreading, a 0.5 cm x 0.5 cm coverslip was placed on top of the drop. The solvent was allowed to evaporate at 4°C for 24 h. The unbound enzyme was removed by rinsing with distilled water.

2.3 Biochemical assay of GOx immobilized films.

Enzyme assay mixture consisted of 2 mL 0.1 M phenol phosphate buffer (pH 7.0), 0.5 mL horse radish peroxidase (25U mL^{-1}), 0.5mL glucose (10% w/v) and 100 µL Amino anti pyrine (AAP) (4mg mL^{-1}). The solution was pre-incubated at 37 °C for 10 minutes, and then the electrode was suspended in the mixture and the absorbance at 500nm was measured every 5 minutes for 30 minutes. The enzyme activity was calculated using the formula

$$\frac{U}{cm^2} = \left(\frac{\Delta OD_{Test}}{Min} - \frac{\Delta OD_{Blank}}{Min}\right) \times \frac{1}{12.88 \times \frac{1}{2}} \times Reaction\ Volume \times \frac{1}{Area\ (cm^2)}$$

Where 1U = enzyme concentration which oxidizes 1µmol of β-D-glucose per minute as per the conditions mentioned above, 12.88 is the milli-molar extinction coefficient of oxidized 4-AAP and the factor ½ corresponds to the two moles of H_2O_2 required to reduce 1 mole of AAP[23].

Protein immobilized on the thin film surface was estimated as per Kang et al[24]. Bradford reagent was prepared by dissolving 50 mg of Coomassie brilliant blue 250 in 50 mL ethanol and 100 mL 88% ortho-phosphoric acid made up to 1000 mL with distilled water. The solution was filtered through Whatman filter paper and used for further assay. The thin film with immobilized enzyme was incubated in 1.5 mL of Bradford reagent for 5 minutes, after which the solution was centrifuged at 10,000 rpm for 30 minutes. The absorbance of the unreacted Bradford reagent in the supernatant was taken at 540 nm. The amount of the protein present on the surface was estimated by using a standard calibration curve using known GOx concentrations.

2.4 X-ray photo electron spectroscopy of GOx/AZO films:

XPS data were collected by Kratos Axis Ultra DLD spectrometer (Kratos Analytical, UK), equipped with mono-chromatized Al X-ray source ($AlK_{\alpha}h\nu$=1486.6eV), operated at 15 mA and 15 kV. The analyzer band-pass energy was 160 eV or 20 eV with a step size of 1 eV or 0.5 eV for the survey or high resolution spectra, respectively. The spot size for analysis was 300 µm x 700 µm in a chamber pressure of 10^{-8} Pa (7.5×10^{-8}mTorr). Deconvolution and analyses of the XPS peaks were performed using the Fityk software[25].

2.5 Electrochemical analyses of GOx immobilized films

In all potentiostat-controlled experiments, Ag/AgCl was used as reference electrode and platinum wire as counter electrode. Copper wire was connected with silver paste to the ZnO thin film side. The connection was kept above the solution in air, carefully avoiding contact with the electrolyte. The area of the working electrode was 0.25 cm^2(0.5 cm x 0.5 cm). All the analyses were done in 0.1M phosphate buffer at pH 7.4 to mimic the physiological buffered conditions of the blood serum.

Schematic: Electrodes suspended in electrochemical set up.

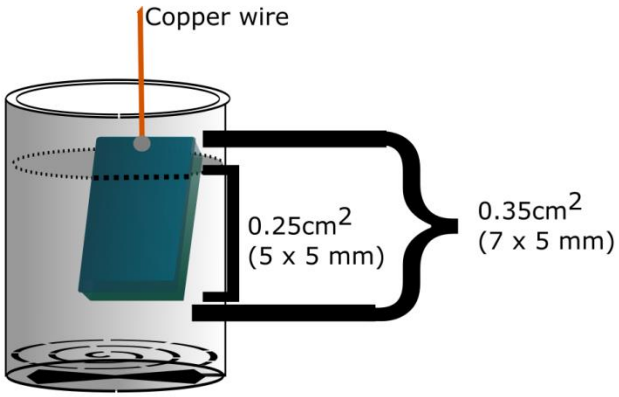

CV, CA and EIS of the enzyme-thin film assembly were carried out using a CH 660A potentiostat (CH Instruments, USA). For CV, the working electrode potential was scanned between +0.8and -0.8V vs. Ag/AgCl. Only the last of the 5 cycles is reported. The scan rate was varied between 10 and 200 mV $s^{-1}$and the glucose concentration was set at 5 mM. In the CA experiments, the enzyme-thin film construct was poised at -0.6 V vs. Ag/AgCl in phosphate buffer (pH=7.2). The glucose calibration curve was obtained by the incremental addition of the glucose from 0 to 28mM and the limiting cathodic (reduction) current was recorded. LoD/LoQ was measured by adding buffer and measuring the change in current.

LoD/LoQ= Standard deviation *(S/N)/sensitivity, ……(Eq. 1)

where S/N is considered as 3 for LoD and 5 for LoQ [26].

For the EIS, the potential and amplitude were set at -0.4 vs. Ag/AgCl and 5 mV, respectively. The frequency range of 1Hz-100 kHz was used. The Nyquist plot obtained was fitted to several well-known equivalent circuits to analyze the electron transfer path using EIS spectrum analyzer with the Powell algorithm [27].

Human Serum Analyses:

Clinical serum samples were obtained with high (10-25 mM) and low (5 – 9 mM) blood glucose level. The analyses were performed by chronoamperometry at -0.6V and stirring of 500 rpm as per condition mentioned above. Dilutions of 1:20 v/v of serum samples were used. After stable current was obtained, the readings were noted. The glucose levels were calculated using the calibration curve of current obtained for glucose by chronoamperometry in the previous experiments (Figure 6). The glucose values were then compared with glucose values obtained in the diagnostic laboratory by automated analyzer using glucose oxidase-peroxidase (GOD-POD) method.

3. Results and discussions

3.1 Characterization of structural, optical & electrical properties of the prepared thin films:

Preliminary screening was done to obtain the optimum oxygen partial pressure (10, 30, 75 mTorr) and Al concentration (0.045, 4.5 atomic %) required for the deposition of high quality films for GOx immobilization and electrochemical analyses. Based on better peaks in CV and electrical properties the conditions for deposition were optimized and for AZO films target containing 4.5 atomic% aluminum was used in all further studies. Figure 1(a) shows the morphologies of the ZnO and AZO films with grain sizes around 20-30 nm. Previous works have shown that ZnO films grown by PLD on glass [28], sapphire [29]and Perspex (or PMMA) [30] and Zeonor [32] plastic substrates have a similar grain morphology. From the XRD pattern, 2θ values for the ZnO and AZO films were seen at around 34.4° (Figure 1b). These values correspond to the (002) reflection of the wurtzite structure (ICSD# 082029), showing a preferred orientation with the *c*-axis perpendicular to the ZnO and AZO films surface. The peak position was similar to that reported previously for ZnO thin films produced by plasma deposition methods [31].The crystallite sizes of the deposited films were measured using Scherrer equation and the results were 38 and 23 nm for ZnO and AZO, respectively [32]. Software analyses (Xpert high score) of the diffraction peak profiles also indicated higher lattice strain for AZO than for ZnO thin film, likely due to Al incorporation in the ZnO lattice.

In Figure 2, the transmission spectra between 200 and 1100 nm of the ZnO and AZO films are presented. The thickness and the optical band gap of the deposited thin films were estimated by fitting the transmission spectra using the Scout 2 software. A non-linear least square-fitting algorithm was used to extract the optical constants of the films, from transmittance data alone, based on a composite model for the complex dielectric function [33]. The model assumes parabolic bands in the UV-vis region and a Drude model in the NIR region. The thicknesses thus obtained for the ZnO and AZO thin films were approximately 132 and 90-100 nm, respectively. The small difference observed for the lower visible transparency of the ZnO films can be accounted for by the thickness difference[33,34]. An independent analysis with surface reflectometry confirmed the above thickness with a surface roughness of 10 nm. The fitted

optical band gaps were 3.24 and 3.35 eV for ZnO and AZO, respectively, in agreement with previous reports [35,36].

The electrical measurements showed that both AZO and ZnO thin films had a sheet resistance in the range of 4000 Ω sq^{-1}, corresponding to a bulk resistivity of about 0.04 Ω cm, indicative of good conductive properties[37]. From the Hall measurements, sheet concentrations of -1.44 x 10^{15} cm^{-2} and -6 x 10^{14} cm^{-2} for the AZO and ZnO thin films, respectively, were obtained. The ZnO films deposited at higher oxygen pressure (75 mTorr) had a sheet concentration of -2.22 x 10^{10} cm^{-2}, whereas low Al doping (0.045 at%) yielded a sheet concentration of -7.2 x 10^{10} cm^{-2}. These results indicate the strong influence of both Al dopant concentration and oxygen growth pressure on the surface carrier concentration. Overall, the electrical measurements confirmed that the AZO and ZnO thin films prepared in this study could be used directly as base electrode even though they are supported on an insulating PC plastic substrate. The prepare films were found to be stable up to the period of 2 years at room temperature.

3.2 Characterization of GOx modified electrode

The enzyme activity and protein concentration assayed on the surface of ZnO thin films were higher than on the AZO films (Figure 3) and comparable to previously reported by Saha et al (2009) (0.029 U cm^{-2}) [23]. In addition, the specific activity of the GOx (U mg^{-1} of protein) obtained by ratio of activity to protein concentration, was found to 0.033 U cm^{-2} AZO thin films surface in comparison to ZnO thin films with 0.043 U cm^{-2}.

The nature of interaction of the enzyme with the thin films was studied using XPS (Figure 4). The survey scan showed the presence of nitrogen after the immobilization of the protein on the thin film surface (Figure 4a). No change in the binding energy of the Zn peaks were seen, which indicates that most of the interaction was with the oxygen of the AZO (Figure 4(a)). After deconvolution (Figure 4(b)) of the measured O1*s* peak, three components were observed at binding energies of 531.6 eV, 533.0 eV and 535.4 eV, which correspond to loosely bound oxygen in ZnO matrix [5,29] or carbonyl, ester and loosely bound hydroxyl groups, respectively[5,38]. The Wurtzite oxygen peak was also observed at 530 eV in GOx/AZO [39]. The interaction of oxygen with the protein may have given rise to the peak at 535.0 eV. On deconvolution of the N peak (Figure 4(c)), two components were observed at 399.2 eV and 400.3 eV, which correspond to amine and amide linkage of the protein, respectively[40]. The peaks corresponding to NH_2 may have contributions from exposed lysine, arginine, and asparagine residues of glucose oxidase, whereas the C-N linkage corresponds to the peptide bonds within the protein. So it can be inferred that the binding of the protein with the surface of the film was due to ionic and dipole interaction between the amine residue of the protein and oxygen moiety of ZnO.

3.3 Kinetics of modified electrodes GOx/ZnO and GOx/AZO

3.3.1 Cyclic Voltammetry of the GOx/AZO and GOx/ZnO electrodes

The CV of the thin films showed a poorly reversible peak at 0.272 and0.286 vs. Ag/AgCl for GOx/ZnO and GOx/AZO at 10 mV $s^{-}1$ scan rate, respectively. The I_p measured from CVs at different scan rates between 10 and 200 mV s^{-1}correlates linearly with the square root of the scan rate, indicating that electron transfer rate is limited by diffusion in the liquid phase (Figure 5(a-b)). The slope of the I_p vs.$v^{0.5}$ plot shows a higher slope for GOx/ZnO as compared to that of GOx/AZO, likely because of the higher enzyme concentration on the ZnO film surface (Figure S1 (a-b)). Plot of E_p vs. log(v) showed a higher ΔE for GOx/ZnO as compared to GOx/AZO, due to the higher conductivity of the AZO films as compared to the ZnO thin film (Figure S1(c-d)). Thus the CV analyses was in agreement with the biochemical and confirmed that the enzyme activity is higher on ZnO than on AZO films. The surface concentration estimated by Brown Anson model was in agreement with the biochemical assay for protein estimation with 1.20 x 10^{-10} mol cm^{-2} for GOx/ZnO/PC and 3.20 x 10^{-12} mol cm^{-2} for GOx/AZO/PC [15].

3.3.2 Calibration curve and Michaelis Menton contant (Km)

The overall reaction mechanism can be summarized as the reduction of H_2O_2 which is a byproduct of glucose oxidation on the surface of the film. As a result for reduction of H_2O_2 the calibration curve was obtained at -0.6 V. The glucose calibration curve measured by CA indicated the sensitivity of GOx/AZO thin films was better (5.5 µA cm^{-2} mM^{-1} of glucose), compared to GOx/ZnO thin films (2.2 µA cm^{-2} mM^{-1} of glucose) (Figure 6b). GOx/AZO thin film showed fast and sensitive response to glucose as it required a period of 10 s to reach the steady state of current (Figure 6a). This higher sensitivity corresponds to the faster rate of reduction of peroxide on the surface of AZO thin films as compared to the ZnO thin films[41,42]. The limiting current is dependent not only on the concentration of the bulk solution but also on the diffusion thickness, which in turn depends on the rate of breakdown of H_2O_2 on the surface of thin films. As mentioned above, AZO films had higher sheet concentration of electrons as measured by the Hall Effect (-1.44 x 10^{15} cm^{-2} for AZO and -6 x 10^{14} cm^{-2} for ZnO). Thus, the high concentration of the electrons could have accounted for more reducing surface allowing faster breakdown of H_2O_2 on AZO thin.

The limit of detection (LoD) was calculated as per Eq 1 mentioned in the Experimental details. For the AZO and ZnO thin films it was calculated to be 160 µM and 367 µM of glucose, respectively. The repeatability of the system was tested by doing CA on a single electrode twice on the next day, which showed reproducible results. Common interfering species such as ascorbic acid, cholesterol, urea & cysteine require a high oxidation potential for detection [43]. It may be inferred that GOx immobilized electrodes does not have interference from the fact that its operation condition is negative potential. The potential used in this study is lower compared to previously reported potentials for sensing in mediated and non-mediated biosensors [44,45]. Since the present study contemplated devising a low cost electrode on an inexpensive substrate PC, only one-time usage was envisaged. But the electrodes were able to produce comparable current even after 48 hours of preparation and 2nd cycle of use (Figure S4).

The sensitivity of GOx/AZO/PC prepared here was higher than GOx immobilized on other substrates without mediator reported in (Table 1). It is also comparable to the complex sensors involving nanomaterials (Table 1). The present work is the first study on GOx immobilized on PLD coated ZnO film on PC without any mediator at neutral pH. The GOx/AZO/PC exhibited a wider linear range of 0.26-28 mM glucose as compared to previous reports (Table 1).

To evaluate the biological activity of the enzyme, the apparent Michaelis-Menten constant (K_m) for the calibration graph was obtained through the Lineweaver-Burke plot (Figure 6(c))[44]

$$\frac{I_{max}}{I_s} = \frac{K_m}{C} + 1$$

Where I_{max} is the maximum current obtained by the system, I_s is the steady state current and C is the concentration of the glucose. K_m was 21.7 mM and 66.7 mM of glucose for GOx/ZnO and GOx/AZO, respectively. This was in agreement with the biochemical assay data which showed higher specific activity of GOx on ZnO as compared to AZO.

3.3.3 Electrochemical Impedance Spectroscopy of prepared and GOx modified electrodes:

The Nyquist plot of thin film only is reported in Table S1, together with the fitting results of its equivalent circuit. The results show only one time constant, as expected for semiconductor under non-turnover conditions. An infinite Warburg element was added to account for diffusion in the solution. These data are consistent with previous literature which shows similar circuit model for deposited ZnO films[50]. As observed from the equivalent circuit fit shown in Figure 7(a), the charge transfer resistance of thin film interface was higher in case of ZnO/PC with 6.95± 0.9 x 10^5 Ω as compared to AZO/PC with 2.21± 0.04 x 10^5 Ω (Table 2). When GOx is coated on the film, a second time constant at higher frequency appears. The charge transfer resistance value were 21.8± 3.3 x 10^4 Ω and 3.7± 0.9 x 10^4 Ω for GOx/ZnO and GOx/AZO, respectively, due to the lower conductivity of ZnO thin film and the higher enzyme loading on the surface of the ZnO/PC as observed from the biochemical assay data (Table 2).The Nyquist plot shows that the charge transfer resistance was higher in GOx/ZnO/PC as compared to GOx/AZO/PC (Figure 7(a)). However, upon addition of glucose, the charge transfer resistance under turnover conditions decreased to similar values for ZnO and AZO thin films (5.6 ± 2.2 x 10^3 Ω and 7.72 ± 0.7 x 10^3 Ω, respectively, Figure 7(b) and Table 2). As observed, the magnitude for the decrease for the GOx catalyzed reaction of glucose is higher in case of GOx/ZnO as compared to that of GOx/AZO. This is in agreement with the Bode plot, which shows a more defined time constant for ZnO/PC as compared to AZO/PC (Figure S3). The detailed fitting parameters of the EIS spectra are provided in the supplementary information (Table S1, S2 & S3).

GOx/ZnO/PC exhibited a better catalytic activity towards glucose as compared to GOx/AZO/PC, due to high enzyme loading rather than the conductivity of the thin film itself. However, GOX/AZO/PC had better sensitivity to glucose with lesser enzyme loading, which may be attributable to the carrier concentration of AZO films.

3.3.4 Validation of glucose sensing using blood serum:

The real time application of the modified electrode was established by analyzing the blood serum sample obtained from diagnostic laboratory (Table 3). The system showed good performance in the higher range of blood sugar with relatively low error compared to values from the diagnostic laboratory. The error for lower range can be further reduced by miniaturization of the electrode with appropriate connection to the signal processor and better fabrication. Thus, the current system is suitable for fabrication of self-diagnostic device with the optimal range in 100-450 mg dl^{-1} of blood glucose level.

4.Conclusions:

A novel approach for immobilizing GOx on a conductive ZnO matrix deposited on a non-conducting base like PC is described here. Increased carrier concentration of the thin film on doping of Al was exploited for easy electron transfer by immobilizing GOx by a simple method of drop casting. Though immobilized protein was decreased on doping, the sensitivity for the detection of glucose was higher compared to un-doped ZnO. It appeared that the dipole interaction of the amino groups of the protein with the oxygen atoms of AZO was the probable basis of interaction. GOx/AZO had a better sensitivity of 5.5 μA cm^{-2} mM^{-1} compared to GOx/ZnO with 2.2 μA cm^{-2} mM^{-1}. GOx/AZO had a wide range of detection of glucose from 0.28-28 mM with LoD of 167 μM and a fast response time of 10s. GOx/AZO also performed better for detecting glucose in real blood with better better accuracy than GOx/ZnO. We envisage that such new doped metal oxide matrices on PC wherein model enzyme like GOx can be easily immobilized would serve as a new platform for the development of the other redox enzyme based biosensors.

Acknowledgments

The authors are thankful for the financial support received under the DST India-Ireland Cooperative Science Program. S. Inguva acknowledges INSPIRE (Integrated Nanoscience Platform for Ireland), PRTLI5, National Development Plan 2007-2013, with the assistance of the European Regional Development Fund.

References:

[1] S.K. Arya, S. Saha, J.E. Ramirez-Vick, V. Gupta, S. Bhansali, S.P. Singh, Recent advances in ZnO nanostructures and thin films for biosensor applications: review., Anal. Chim. Acta. 737 (2012) 1–21. doi:10.1016/j.aca.2012.05.048.

[2] J.X. Wang, X.W. Sun, a. Wei, Y. Lei, X.P. Cai, C.M. Li, et al., Zinc oxide nanocomb biosensor for glucose detection, Appl. Phys. Lett. 88 (2006) 233106. doi:10.1063/1.2210078.

[3] Z. Dai, G. Shao, J. Hong, J. Bao, J. Shen, Immobilization and direct electrochemistry of glucose oxidase on a tetragonal pyramid-shaped porous ZnO nanostructure for a glucose biosensor, Biosens. Bioelectron. 24 (2009) 1286–1291. doi:10.1016/j.bios.2008.07.047.

[4] A. Janotti, C.G. Van de Walle, Fundamentals of zinc oxide as a semiconductor, Reports Prog. Phys. 72 (2009) 126501. doi:10.1088/0034-4885/72/12/126501.

[5] Z.L. Wang, Novel nanostructures of ZnO for nanoscale photonics, optoelectronics, piezoelectricity, and sensing, Appl. Phys. A. 88 (2007) 7–15. doi:10.1007/s00339-007-3942-8.

[6] Y. Liu, Y. Li, H. Zeng, ZnO-Based Transparent Conductive Thin Films : Doping , Performance , and Processing, J. Nanomater. 2013 (2013) 9. doi:10.1155/2013/196521.

[7] S.-C. Chang, Post-annealed gallium and aluminum co-doped zinc oxide films applied in organic photovoltaic devices, Nanoscale Res. Lett. 9 (2014) 562. doi:10.1186/1556-276X-9-562.

[8] M.-C. Jun, S.-U. Park, J.-H. Koh, Comparative studies of Al-doped ZnO and Ga-doped ZnO transparent conducting oxide thin films., Nanoscale Res. Lett. 7 (2012) 639. doi:10.1186/1556-276X-7-639.
[9] H. Hagendorfer, K. Lienau, S. Nishiwaki, C.M. Fella, L. Kranz, A.R. Uhl, et al., Highly transparent and conductive ZnO: Al thin films from a low temperature aqueous solution approach, Adv. Mater. 26 (2014) 632–636. doi:10.1002/adma.201303186.
[10] E.L. Papadopoulou, M. Varda, K. Kouroupis-Agalou, M. Androulidaki, E. Chikoidze, P. Galtier, et al., Undoped and Al-doped ZnO films with tuned properties grown by pulsed laser deposition, Thin Solid Films. 516 (2008) 8141–8145. doi:10.1016/j.tsf.2008.04.022.
[11] A.C. Aragonès, A. Palacios-Padrós, F. Caballero-Briones, F. Sanz, Study and improvement of aluminium doped ZnO thin films: Limits and advantages, Electrochim. Acta. 109 (2013) 117–124. doi:10.1016/j.electacta.2013.07.053.
[12] N.D. Md Sin, M. Fuad Kamel, R.I. Alip, Z. Mohamad, M. Rusop, The electrical characteristics of aluminium doped zinc oxide thin film for humidity sensor applications, Adv. Mater. Sci. Eng. 2011 (2011). doi:10.1155/2011/974906.
[13] M. Hjiri, L. Mir, S. Leonardi, Synthesis, Characterization and Sensing Properties of AZO and IZO Nanomaterials, Chemosensors. 2 (2014) 121–130. doi:10.3390/chemosensors2020121.
[14] S. Saha, V. Gupta, Al and Fe co-doped transparent conducting ZnO thin film for mediator-less biosensing application, AIP Adv. 1 (2011) 42112. doi:10.1063/1.3654497.
[15] J. Singh, M. Srivastava, A. Roychoudhury, D.W. Lee, S.H. Lee, B.D. Malhotra, Bienzyme-functionalized monodispersed biocompatible cuprous oxide/chitosan nanocomposite platform for biomedical application, J. Phys. Chem. B. 117 (2013) 141–152. doi:10.1021/jp309639w.
[16] J. Singh, P. Kalita, M.K. Singh, B.D. Malhotra, Nanostructured nickel oxide-chitosan film for application to cholesterol sensor, Appl. Phys. Lett. 98 (2011) 12–15. doi:10.1063/1.3553765.
[17] J. Singh, P. Khanra, T. Kuila, M. Srivastava, A.K. Das, N.H. Kim, et al., Preparation of sulfonated poly(ether-ether-ketone) functionalized ternary graphene/AuNPs/chitosan nanocomposite for efficient glucose biosensor, Process Biochem. 48 (2013) 1724–1735. doi:10.1016/j.procbio.2013.07.025.
[18] A.R. Schlatmann, D.W. Floet, A. Hilberer, F. Garten, P.J.M. Smulders, T.M. Klapwijk, et al., Indium contamination from the indium–tin–oxide electrode in polymer light-emitting diodes, Appl. Phys. Lett. 69 (1996) 1764. doi:10.1063/1.117478.
[19] Y. Liu, L. Zhao, J. Lian, Al-doped ZnO films by pulsed laser deposition at room temperature, Vacuum. 81 (2006) 18–21. doi:10.1016/j.vacuum.2006.02.001.
[20] T. Kwan Chu, L. Yen Sian, Y. Seong Ling, K. Soon Yie, N. Chen Hon, S. Wee Ong, et al., Pulsed laser deposition of Al-doped ZnO films on glass and polycarbonate, J. Nanophotonics. (2014) 8. http://spie.org/Publications/Journal/10.1117/1.JNP.8.084091 (accessed September 14, 2015).
[21] R. Wilson, A.P.F. Tuner, Review article Glucose oxidase : an ideal enzyme, Biosens. Bioelectron. 7 (1992) 165–185. http://linkinghub.elsevier.com/retrieve/pii/S0308814600001278.
[22] M.M. Rahman, a J. Saleh Ahammad, J.-H. Jin, S.J. Ahn, J.-J. Lee, A comprehensive review of glucose biosensors based on nanostructured metal-oxides., Sensors (Basel). 10 (2010) 4855–86. doi:10.3390/s100504855.

[23] S. Saha, S.K. Arya, S.P. Singh, K. Sreenivas, B.D. Malhotra, V. Gupta, Nanoporous cerium oxide thin film for glucose biosensor., Biosens. Bioelectron. 24 (2009) 2040–5. doi:10.1016/j.bios.2008.10.032.
[24] I. Kang, B.K. Kwon, J.H. Lee, H.B. Lee, Immobilization of proteins on polyl(methyl methacrylate) films, Biomaterials. 14 (1993) 787–792.
[25] M. Wojdyr, Fityk : a general-purpose peak fitting program, J. Appl. Crystallogr. 43 (2010) 1126–1128. doi:10.1107/S0021889810030499.
[26] A. Ullah, A. Rauf, U.A. Rana, R. Qureshi, M.N. Ashiq, H. Hussain, et al., pH Dependent Electrochemistry of Anthracenediones at a Glassy Carbon Electrode, J. Electrochem. Soc. 162 (2015) H157–H163. doi:10.1149/2.0881503jes.
[27] Bondarenko, R. G., Inverse Problem In Potentiodynamic Electrochemical Impedance, Prog. Chemom. Res. (2005) 89–102. https://www.novapublishers.com/catalog/product_info.php?products_id=2337 (accessed September 14, 2015).
[28] J. Mosnier, R.J.O. Haire, E. Mcglynn, O. Martin, ZnO films grown by pulsed-laser deposition on soda lime glass substrates for the ultraviolet inactivation of Staphylococcus epidermidis biofilms, Sci. Technol. Adv. Mater. 45003 (2009). doi:10.1088/1468-6996/10/4/045003.
[29] R. O'Haire, E. McGlynn, M.O. Henry, J.-P. Mosnier, ZnO nanostructured thin films grown by pulsed laser deposition in mixed O2 / Ar background gas, Superlattices Microstruct. 42 (2007) 468–472. doi:10.1016/j.spmi.2007.04.020.
[30] J. Connolly, A. Jain, G. Pastorella, S. Krishnamurthy, J.-P. Mosnier, E. Marsili, Zinc oxide and indium tin oxide thin films for the growth and characterization of Shewanella loihica PV-4 electroactive biofilms, Virulence, (2011), 489-90. http://www.tandfonline.com/doi/abs/10.4161/viru.2.5.17912#.VfY4B33A3cu (accessed September 14, 2015).
[31] S. Inguva, R.K. Vijayaraghavan, E. McGlynn, J.-P. Mosnier, Highly transparent and reproducible nanocrystalline ZnO and AZO thin films grown by room temperature pulsed-laser deposition on flexible Zeonor plastic substrates, Mater. Res. Express. 2 (2015) 96401. doi:10.1088/2053-1591/2/9/096401.
[32] A. Djelloul, K. Bouzid, F. Guerrab, C.U.K. Erie, Role of Substrate Temperature on the Structural and Morphological Properties of ZnO Thin Films Deposited by Ultrasonic Spray Pyrolysis, Turkish J. Phys. 32 (2008) 49–58.
[33] W. Theiss, Hard-and Software for Optical Spectroscopy: Compute optical constants of substrates from R and T spectra Part I Overview 2, 2007. www.mtheiss.com (accessed September 9, 2016).
[34] B.L. Zhu, X.Z. Zhao, S. Xu, F.H. Su, G.H. Li, X.G. Wu, et al., Oxygen Pressure Dependences of Structure and Properties of ZnO Films Deposited on Amorphous Glass Substrates by Pulsed Laser Deposition, Jpn. J. Appl. Phys. 47 (2008) 2225–2229. doi:10.1143/JJAP.47.2225.
[35] P. Gondoni, M. Ghidelli, F. Di Fonzo, M. Carminati, V. Russo, A. Li Bassi, et al., Structure-dependent optical and electrical transport properties of nanostructured Al-doped ZnO., Nanotechnology. 23 (2012) 365706. doi:10.1088/0957-4484/23/36/365706.
[36] H. Kim, A. Piqué, J.. Horwitz, H. Murata, Z.. Kafafi, C.. Gilmore, et al., Effect of aluminum doping on zinc oxide thin films grown by pulsed laser deposition for organic light-emitting devices, Thin Solid Films. 377–378 (2000) 798–802. doi:10.1016/S0040-

6090(00)01290-6.
[37] J.G. Lu, Z.Z. Ye, Y.J. Zeng, L.P. Zhu, L. Wang, J. Yuan, et al., Structural, optical, and electrical properties of (Zn,Al)O films over a wide range of compositions, J. Appl. Phys. 100 (2006) 1–11. doi:10.1063/1.2357638.
[38] D.M. Eby, K. Artyushkova, A.K. Paravastu, G.R. Johnson, Probing the molecular structure of antimicrobial peptide-mediated silica condensation using X-ray photoelectron spectroscopy, J. Mater. Chem. 22 (2012) 9875. doi:10.1039/c2jm30837a.
[39] U. Ilyas, R.S. Rawat, T.L. Tan, P. Lee, R. Chen, H.D. Sun, et al., Oxygen rich p-type ZnO thin films using wet chemical route with enhanced carrier concentration by temperature-dependent tuning of acceptor defects, J. Appl. Phys. 110 (2011) 1–7. doi:10.1063/1.3660284.
[40] J.G.H. and C. Chaiwong, S Sarapirom , J S Lee , S B Jin, D H Song , L D Yu, Wettability Effect of PECVD-SiO x Films on Poly(lactic acid) Induced by Oxygen Plasma on Protein Adsorption and Cell Attachment, J. Phys. Conf. Ser. 423 (2013) 12042. doi:10.1088/1742-6596/423/1/012042.
[41] M.R. Guascito, E. Filippo, C. Malitesta, D. Manno, A. Serra, A Turco, A new amperometric nanostructured sensor for the analytical determination of hydrogen peroxide., Biosens. Bioelectron. 24 (2008) 1063–9. doi:10.1016/j.bios.2008.07.048.
[42] A. a. Ensafi, M. Jafari-Asl, N. Dorostkar, M. Ghiaci, M.V. Martínez-Huerta, J.L.G. Fierro, The fabrication and characterization of Cu-nanoparticle immobilization on a hybrid chitosan derivative-carbon support as a novel electrochemical sensor: application for the sensitive enzymeless oxidation of glucose and reduction of hydrogen peroxide, J. Mater. Chem. B. 2 (2014) 706. doi:10.1039/c3tb21434f.
[43] T. Kong, Y. Chen, Y. Ye, K. Zhang, Z. Wang, X. Wang, An amperometric glucose biosensor based on the immobilization of glucose oxidase on the ZnO nanotubes, Sensors Actuators B Chem. 138 (2009) 344–350. doi:10.1016/j.snb.2009.01.002.
[44] R. Ramya, M. V Sangaranarayanan, Electrochemical Sensing of Glucose Using Polyaniline Nanofiber Dendrites-Amperometric and Impedimetric Analysis, J. Appl. Polym. Sci. 129 (2013) 735–747. doi:10.1002/app.38770.
[45] J. Xie, S. Wang, L. Aryasomayajula, V.K. Varadan, Platinum decorated carbon nanotubes for highly sensitive amperometric glucose sensing, Nanotechnology. 18 (2007) 65503. doi:10.1088/0957-4484/18/6/065503.
[46] S. Saha, S.K. Arya, S.P. Singh, K. Sreenivas, B.D. Malhotra, V. Gupta, Zinc oxide-potassium ferricyanide composite thin film matrix for biosensing applications., Anal. Chim. Acta. 653 (2009) 212–6. doi:10.1016/j.aca.2009.09.002.
[47] F. Hu, S. Chen, C. Wang, R. Yuan, Y. Chai, Y. Xiang, et al., ZnO nanoparticle and multiwalled carbon nanotubes for glucose oxidase direct electron transfer and electrocatalytic activity investigation, J. Mol. Catal. B Enzym. 72 (2011) 298–304. doi:10.1016/j.molcatb.2011.07.005.
[48] S. Saha, V. Gupta, Influence of surface defects in ZnO thin films on its biosensing response characteristic, J. Appl. Phys. 110 (2011) 64904-1–9. doi:10.1063/1.3633212.
[49] X. Ren, D. Chen, X. Meng, F. Tang, X. Hou, D. Han, et al., Zinc oxide nanoparticles/glucose oxidase photoelectrochemical system for the fabrication of biosensor., J. Colloid Interface Sci. 334 (2009) 183–7. doi:10.1016/j.jcis.2009.02.043.
[50] S. Saha, S.K. Arya, S.P. Singh, V. Gupta, A Novel ZnO-Methylene Blue Nanocomposite Matrix for Biosensing Application, Int. J. Electrochem. 2011 (2011) 1–6.

doi:10.4061/2011/823734.

Appendices:

I. Figures:

a. Fig.1(a) SEM morphology of the nanostructured AZO film, Inset shows ZnOfilms;(b) 2θ XRD scans of the ZnO and AZO films.

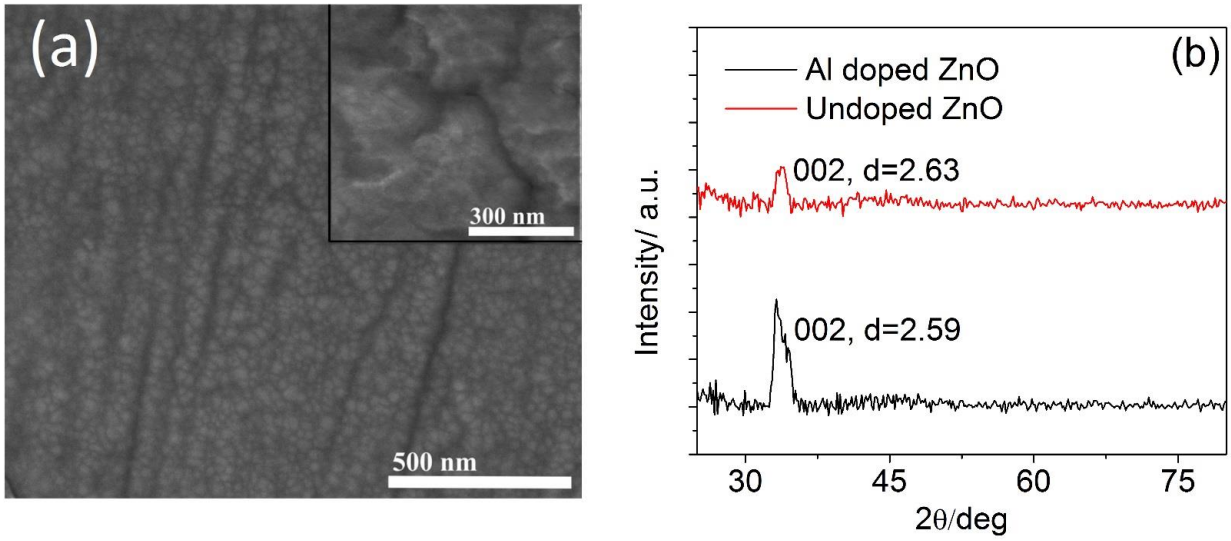

b. Fig.2: Measured and fitted optical transmission spectra of ZnO thin films and AZO thin films.

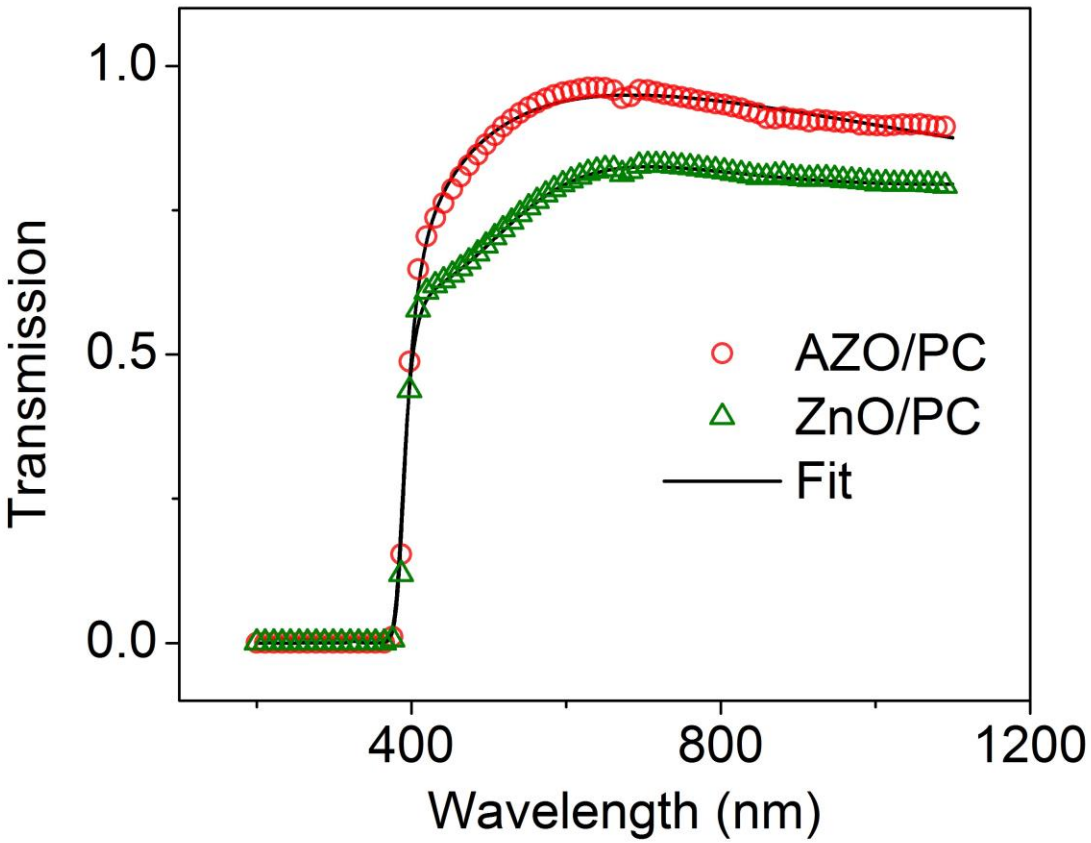

c. Fig.3 Biochemical assay of immobilized GOx on ZnO and AZO thin films. (a) Enzyme activity; (b) Protein concentration.

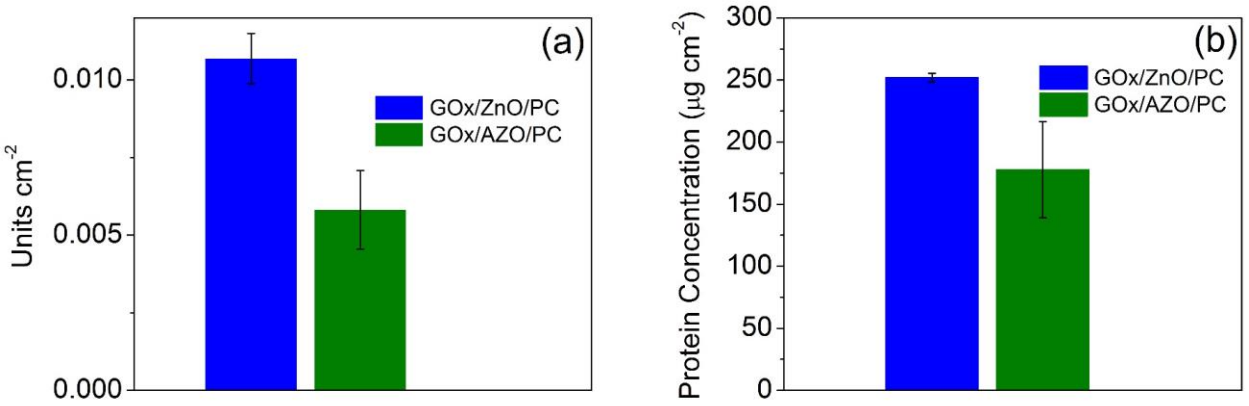

d. Fig.4 XPS of GOx/AZO/PC (a) Survey scan of GOX/AZO/PC and AZO/PC; (b) Deconvolved high resolution peak of O 1*s*; (c) Deconvolved high resolution peak of N 1*s*.

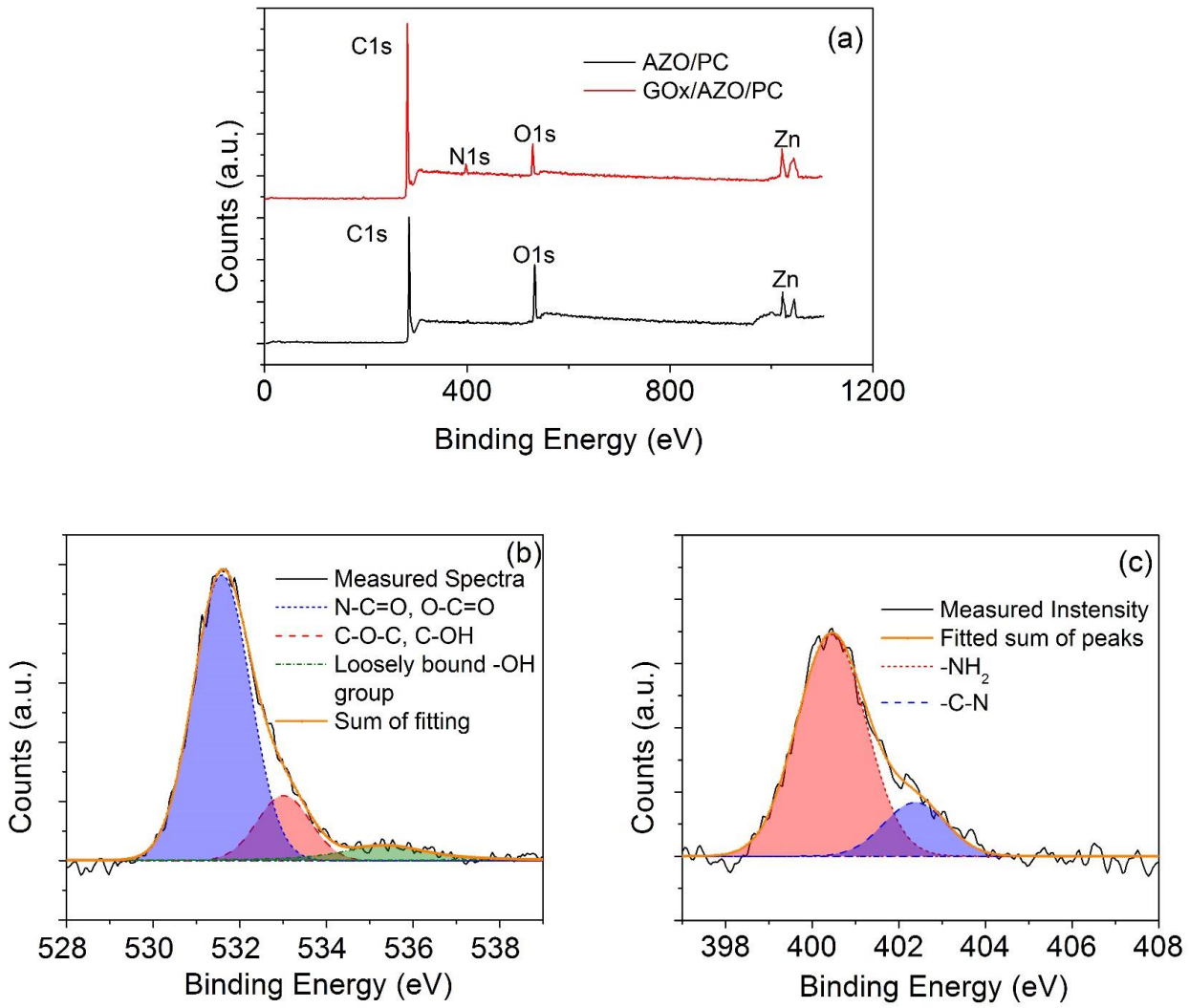

e. Fig. 5 CV of immobilized GOx in 5 mM glucose phosphate buffered (pH7.2).(a) GOx/ZnO/PC; (b) GOx/AZO/PC.

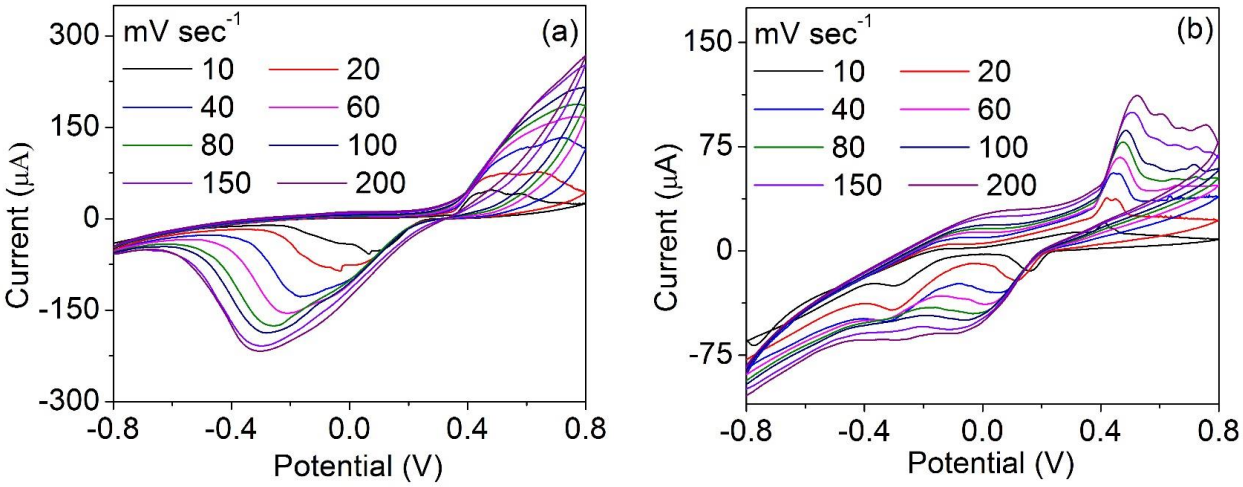

f. Fig. 6(a) Chronoamperogram obtained by incremental addition of glucose (i) GOx/ZnO/PC, (ii) GOx/AZO/PC (b) Amperometric calibration of glucose for GOx immobilized on ZnO/AZO thin films in phosphate buffer (pH-7.2); (c) Lineweaver-Burke plot of amperometric calibration curve.

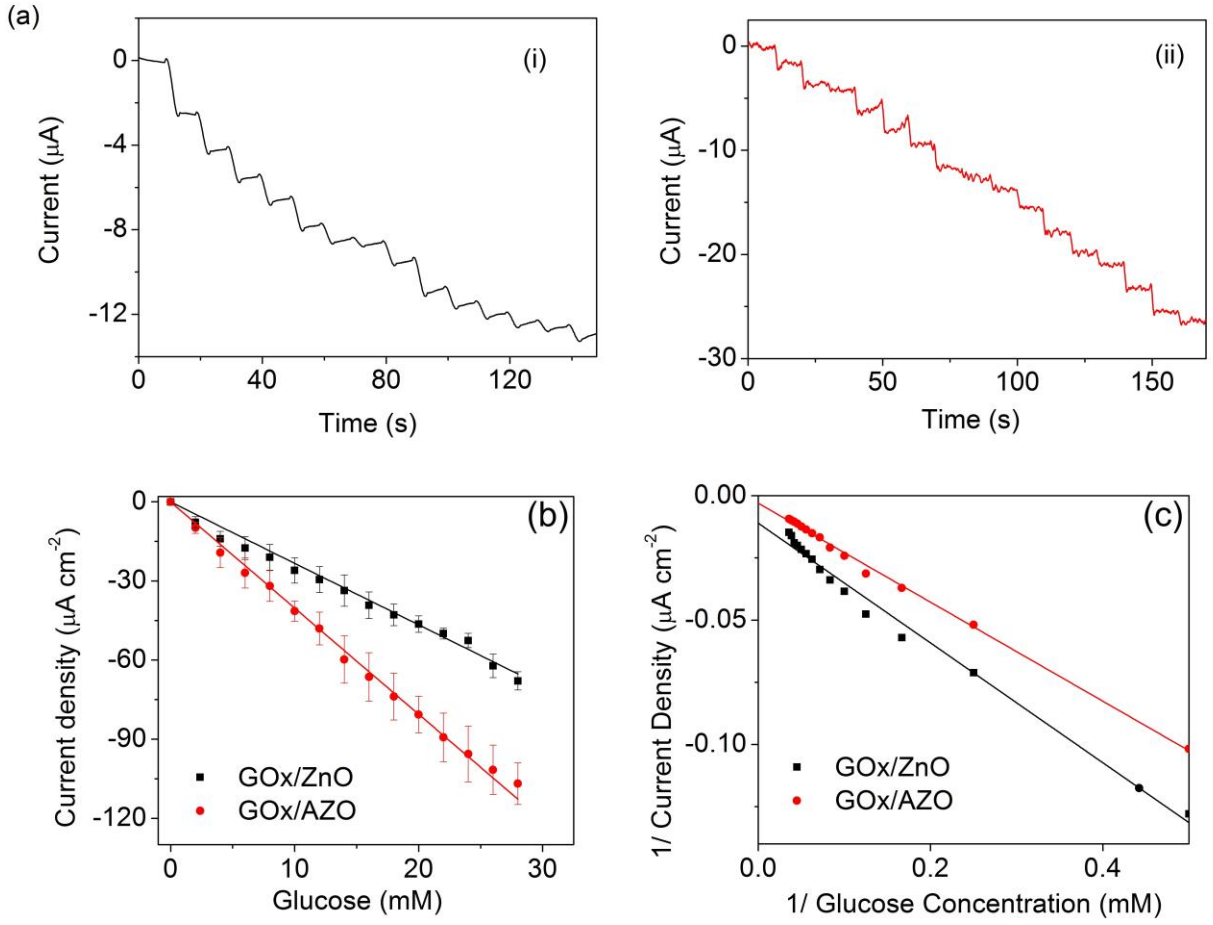

g. Fig. 7 Nyquist plot for (a) GOx/AZO and GOx/ZnO in 0.1M phosphate buffer pH7.2; (b) 5 mM glucose in 0.1M phosphate buffer pH7.2 on GOx/AZO and GOx/ZnO. Inset showing the equivalent circuit model used for the fit.

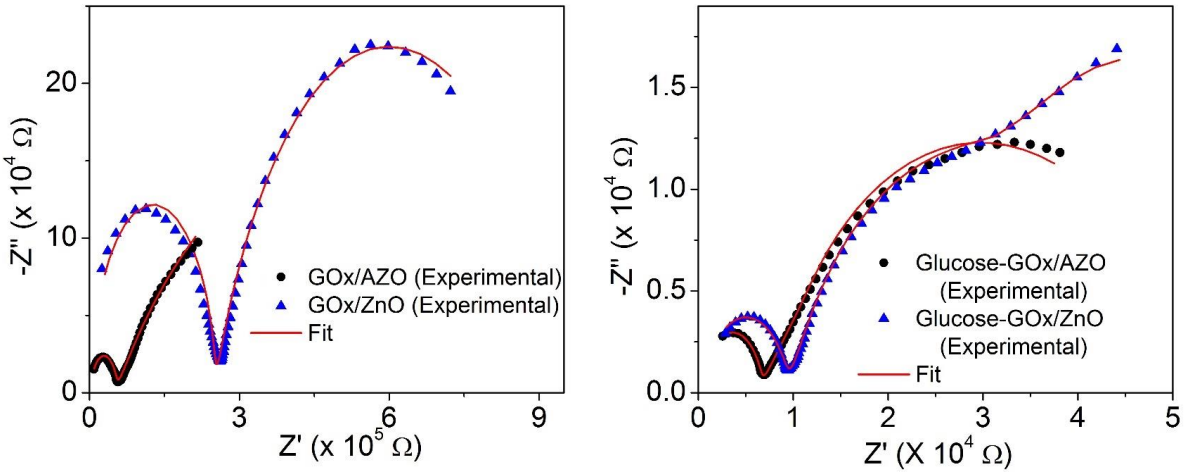

II. Tables:

a. Table 1: Comparison with other mediated and non-mediated glucose sensors
b. Table 2: Charge transfer resistances obtained by fitting of EIS spectra
c. Table 3: Detection of glucose in blood serum sample

Table 1: Comparison with other mediated and non-mediated glucose sensors

System	**Sensitivity (**μA mM^{-1} cm^{-2}**)**	**LoD (**μM**)**	**Range (mM)**	**Ref**
GOx/ZnO–KFCN/ITO/glass	0.078	230	2.78-11.11	[46]
GOx/ZnO/GOx/MWCNTs/GCE	10	2.22	0.007 to 1.29	[47]
GOx/SPG–AuNPs–CH/ITO	6.51	130	0.5-22.2	[17]
ZnO/GOx/ Ferricyanide	1.27	50	1.38 to 22.22	[48]
GOx/ZnO nps/Pt	2.1	5.6	-	[49]
GOx/ZnO-MB/ITO	0.2	-	2.78-16.67	[50]
GOx/AZO/PC	5.5	160	0.26-28	Current Work
GOx/ZnO/PC	2.2	367	0.6-28	

Table 2: Charge transfer resistances obtained by fitting of EIS spectra:

Electrode system	Charge transfer resistance (R_{ct} Ω)
AZO/PC in Buffer	$2.21 \pm 0.04 \times 10^5$
ZnO/PC in Buffer	$6.95 \pm 0.9 \times 10^5$
GOx/AZO/PC in Buffer (non-turnover)	$3.7 \pm 0.9 \times 10^4$
GOx/ZnO/PC in Buffer (non-turnover)	$21.8 \pm 3.3 \times 10^4$
GOx/ZnO/PC in 5mM Glucose (turnover)	$7.72 \pm 0.7 \times 10^3$
GOx/ZnO/PC in 5mM Glucose (turnover)	$5.6 \pm 2.2 \times 10^3$

Table 3: Detection of glucose in blood serum sample:

Clinical Value (mM)	**GOx/AZO/PC (mM)**	**Relative error (%)**	**GOx/ZnO/PC (mM)**	**Relative error (%)**
4.77	5.35	12	6.27	31
7.05	5.8	17.5	6.15	12.8
17	17.7	4.25	18.5	9
23.7	23.28	2.08	25.81	8.58
26.8	28.4	5.65	28.2	4.94